

# Matrix-Isolation Infrared Spectroscopic and Density Functional Theory Studies on Reactions of Laser-Ablated Lead and Tin Atoms with Water Molecules

Yun-Lei Teng,<sup>1,2</sup> Ling Jiang,<sup>1,2</sup> Song Han,<sup>1</sup> and Qiang Xu<sup>\*1,2</sup>

<sup>1</sup>National Institute of Advanced Industrial Science and Technology (AIST), Ikeda, Osaka 563-8577

<sup>2</sup>Graduate School of Engineering, Kobe University, Nada-ku, Kobe 657-8501

Received May 31, 2007; E-mail: q.xu@aist.go.jp

Reactions of laser-ablated lead and tin atoms with water molecules in excess argon were studied by infrared spectroscopy. Insertion products HMOH and HMO ( $M = \text{Pb}$  and  $\text{Sn}$ ) formed in the present experiments and characterized using infrared spectroscopy on the basis of the results of isotopic shifts, mixed isotopic splitting patterns, stepwise annealing, changes in reagent concentration and laser energy, and a comparison with theoretical predictions. Density functional theory calculations were performed on these molecules and the corresponding transition states. Agreement between the experimental and calculated vibrational frequencies, relative absorption intensities, and isotopic shifts supports the identification of these molecules from the matrix infrared spectra. Plausible reaction mechanisms have been proposed to account for the formation of these molecules.

The interactions of metals with water molecules are of considerable interest from academic and industrial viewpoints and have attracted experimental and theoretical attention, because of their important roles in a wide variety of areas, such as catalytic synthesis, surface chemistry, and biochemical systems.<sup>1–11</sup> Many efforts have been made to explore the interaction of  $\text{H}_2\text{O}$  with clean and preadsorbed single crystal metal surfaces and real catalyst surfaces.<sup>1,2</sup> Previous matrix-isolation infrared spectroscopic studies have shown that early transition metal atoms react with water molecules to form initially insertion products spontaneously on annealing, whereas late transition metal atoms react with water molecules to form metal–water adducts.<sup>5–9</sup> Recently, it has been found that Nd, Sm, and Eu atoms react with water molecules to form metal–water adduct complexes and HMOH insertion molecules in solid argon,<sup>10</sup> whereas for U and Th, the insertion  $\text{H}_2\text{UO}$  and  $\text{H}_2\text{ThO}$  molecules, respectively, are generated.<sup>11</sup>

Many efforts have been made to investigate group 14 metal–water complexes and group 14 metal hydroxides. For instance, argon matrix investigations of the reactions of thermally evaporated Si, Ge, Sn, and Pb atoms with water molecules have suggested the formation of  $\text{M}(\text{H}_2\text{O})$  ( $M = \text{Si}$ , Ge, Sn, and Pb), HMOH ( $M = \text{Si}$ , Ge, and Sn),  $\text{HMOH}(\text{H}_2\text{O})$  ( $M = \text{Si}$  and Ge), and  $\text{HM}_2\text{OH}$  ( $M = \text{Ge}$  and Sn) complexes.<sup>5a</sup> However, there are no isotopic substitution experiments and theoretical calculations to support the assignments, and it seems that some assignments for the previously reported IR bands require confirmation. The electronic absorption spectra of  $\text{M}(\text{H}_2\text{O})$  ( $M = \text{Si}$ , Ge, Sn, and Pb) and HMOH ( $M = \text{Si}$ , Ge, and Sn) complexes have also been observed in the electronic matrix-isolation spectroscopic studies.<sup>5b</sup> In addition, lead and tin hydroxides  $\text{M}(\text{OH})$ ,  $\text{M}(\text{OH})_2$ , and  $\text{M}(\text{OH})_4$  ( $M = \text{Pb}$  and Sn) have been found in the reaction of laser-ablated Pb and Sn atoms with  $\text{H}_2\text{O}_2$  in excess argon.<sup>12</sup> Recently, we have reported

the reaction of laser-ablated Ge atoms with water molecules and the characterization of the adduct and insertion products, such as  $\text{Ge}(\text{H}_2\text{O})$ ,  $\text{HGeOH}$ ,  $\text{HGeO}$ ,  $\text{H}_2\text{GeO}$ ,  $\text{GeOH}$ ,  $\text{Ge}(\text{OH})_2$ ,  $\text{HGeOGeH}$ , and  $\text{HGeGeO}$ .<sup>5d</sup>

Recent studies have shown that, with the aid of isotopic substitution techniques, matrix isolation infrared spectroscopy combined with quantum chemical calculation is very powerful for investigating structure and bonding of novel species.<sup>13,14</sup> Here, we report our results for the reactions of water molecules with lead and tin atoms in a solid-argon matrix. IR spectroscopy and theoretical calculations provide evidence for the formation of insertion molecules HMOH and HMO ( $M = \text{Pb}$  and Sn).

## Experimental and Theoretical Methods

The experiment for laser ablation and matrix-isolation infrared spectroscopy was similar to those previously reported.<sup>14</sup> Briefly, a Nd:YAG laser fundamental (1064 nm, 10 Hz repetition rate with 10 ns pulse width) was focused on rotating Pb and Sn targets. The laser-ablated Pb and Sn atoms were co-deposited with  $\text{H}_2\text{O}$  in excess argon onto a CsI window cooled normally to 4 K by means of a closed-cycle helium refrigerator. Typically, a 1–10 mJ pulse<sup>−1</sup> laser power was used.  $\text{H}_2\text{O}$ ,  $\text{H}_2^{18}\text{O}$  (96%  $^{18}\text{O}$ ), and  $\text{D}_2\text{O}$  were subjected to several freeze–pump–thaw cycles before use. In general, matrix samples were deposited for 30–60 min with a typical rate of 2–4 mmol per hour. After sample deposition, IR spectra were recorded on a BIO-RAD FTS-6000e spectrometer at 0.5 cm<sup>−1</sup> resolution using a liquid-nitrogen-cooled HgCdTe (MCT) detector for the spectral range of 5000–400 cm<sup>−1</sup>. Samples were annealed at different temperatures and subjected to broadband irradiation ( $\lambda > 250$  nm) using a high-pressure mercury arc lamp (Ushio, 100 W).

Quantum chemical calculations were performed to predict the structures and vibrational frequencies of the observed reaction products using the Gaussian 03 program.<sup>15</sup> The B3LYP density

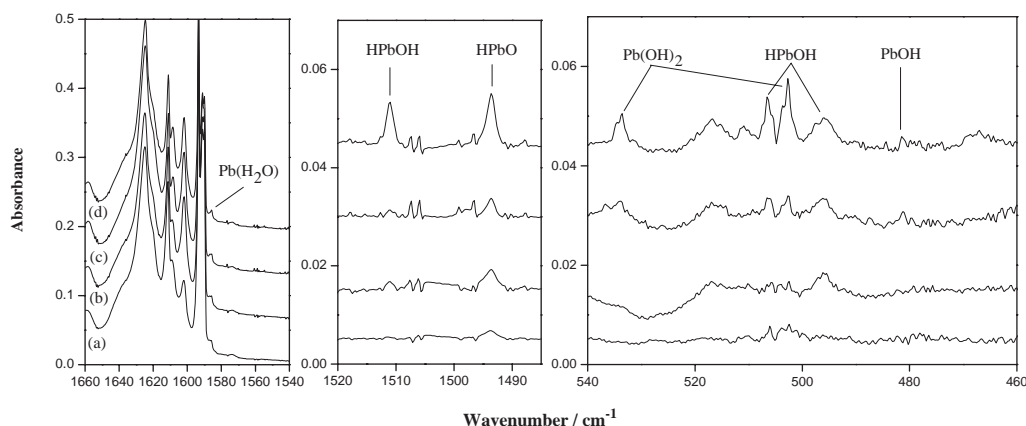


Fig. 1. Infrared spectra in the 1520–1480 and 540–460  $\text{cm}^{-1}$  regions from co-deposition of laser-ablated Pb atoms with 1.0%  $\text{H}_2\text{O}$  in argon: (a) 1 h sample deposition at 4 K; (b) after annealing to 25 K; (c) after 20 min of broad-band irradiation; (d) after annealing to 30 K.

functional method was utilized.<sup>16</sup> The 6-311++G(d, p) basis set was used for H and O atoms, and Los Alamos ECP Plus DZ (LANL2DZ) for Pb and Sn.<sup>8,12,17</sup> Previous investigations have shown that such computational methods can provide reliable information for the Pb and Sn containing molecules, such as infrared frequencies, relative absorption intensities, and isotopic shifts.<sup>18</sup> Geometries were fully optimized and vibrational frequencies were calculated with analytical second derivatives. Transition-state optimizations were done with the synchronous transit-guided quasi-Newton (STQN) method, followed by the vibrational calculations showing the obtained structures to be true saddle points. The intrinsic reaction coordinate (IRC) method was used to track minimum energy paths from transition structures to the corresponding local minima.

### Results and Discussion

Experiments were done with  $\text{H}_2\text{O}$  concentrations ranging from 0.1% to 2.0% in excess argon. Typical infrared spectra for the reactions of laser-ablated Pb and Sn atoms with  $\text{H}_2\text{O}$  molecules in excess argon in the selected regions are illustrated in Figs. 1–6, and the absorption bands are listed in Table 1. The stepwise annealing and irradiation behaviors of these product absorptions are also shown in the figures and will be discussed below.

Quantum chemical calculations were carried out for the possible isomers and electronic states of the potential product molecules. Figure 7 shows the optimized structures and electronic ground states. Table 2 reports a comparison of the observed and calculated IR frequencies and isotopic frequency ratios of the reaction products. Calculated vibrational frequencies and intensities of the potential products are listed in Table 3.

**M( $\text{H}_2\text{O}$ ).** In the Pb +  $\text{H}_2\text{O}$  experiment, an absorption at  $1585.8\text{ cm}^{-1}$  appeared during sample deposition and changed little on annealing and after broad-band irradiation. Although this band has been observed previously,<sup>5a</sup> here, we present a more detailed discussion. It shifted to  $1171.7\text{ cm}^{-1}$  with  $\text{D}_2\text{O}$  and to  $1579.3\text{ cm}^{-1}$  with  $\text{H}_2^{18}\text{O}$ , giving an isotopic H/D ratio of 1.3534 and  $^{16}\text{O}/^{18}\text{O}$  ratio of 1.0041. The band position and isotopic shifts are characteristic of the  $\text{H}_2\text{O}$  bending vibration of a  $\text{H}_2\text{O}$  complex perturbed by a metal atom. No intermediate

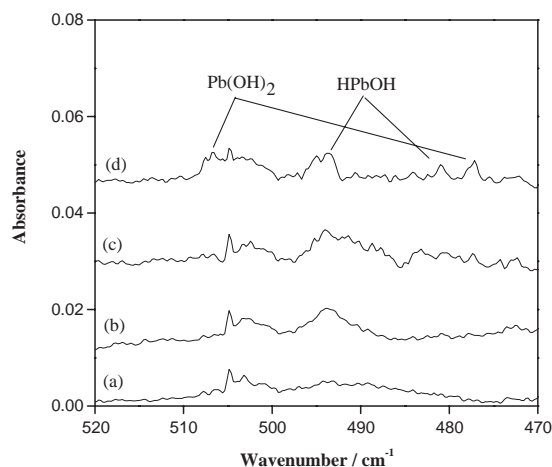


Fig. 2. Infrared spectra in the 520–470  $\text{cm}^{-1}$  region from co-deposition of laser-ablated Pb atoms with 1.0%  $\text{H}_2^{18}\text{O}$  in argon: (a) 1 h sample deposition at 4 K; (b) after annealing to 25 K; (c) after 20 min of broad-band irradiation; (d) after annealing to 30 K.

absorptions were observed in the mixed  $\text{H}_2^{16}\text{O}$  +  $\text{H}_2^{18}\text{O}$  experiments, indicating that only one  $\text{H}_2\text{O}$  subunit is involved in this complex. This band was assigned to the  $\text{H}_2\text{O}$  bending vibration of the  $\text{Pb}(\text{H}_2\text{O})$  complex, which is in agreement with the previous thermal matrix isolation study in solid argon ( $1583.3\text{ cm}^{-1}$ ).<sup>5a</sup>

Density functional theory (DFT) calculations predict the  $\text{Pb}(\text{H}_2\text{O})$  complex to have an  $^3\text{A}''$  electronic ground state with a  $\text{C}_s$  structure, as shown in Fig. 7. The  $\text{H}_2\text{O}$  bending vibrational frequency was calculated to be  $1613.3\text{ cm}^{-1}$  (Table 3), which should be scaled by 0.9830 (observed frequency divided by calculated frequency) to fit the experimental frequency. The calculated isotopic frequency ratios are also in agreement with the experimental values (Table 2).

In the Sn +  $\text{H}_2\text{O}$  experiment, the  $1577.4\text{ cm}^{-1}$  band appeared during sample deposition, markedly increased on sample annealing to 25 and 30 K, disappeared after broad-band irradiation, while the absorption at  $810.6\text{ cm}^{-1}$  due to  $\text{SnO}^{5a}$  markedly increased, and did not recover on further annealing

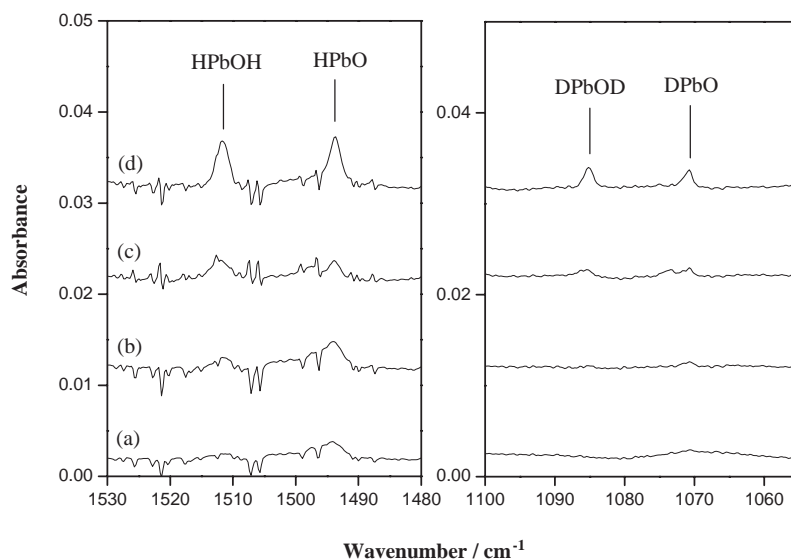


Fig. 3. Infrared spectra in the 1530–1480 and 1100–1155  $\text{cm}^{-1}$  regions from co-deposition of laser-ablated Pb atoms with 0.3%  $\text{H}_2\text{O}$  + 0.6%  $\text{HDO}$  + 0.3%  $\text{D}_2\text{O}$  in argon: (a) 1 h sample deposition at 4 K; (b) after annealing to 25 K; (c) after 20 min of broad-band irradiation; (d) after annealing to 30 K.

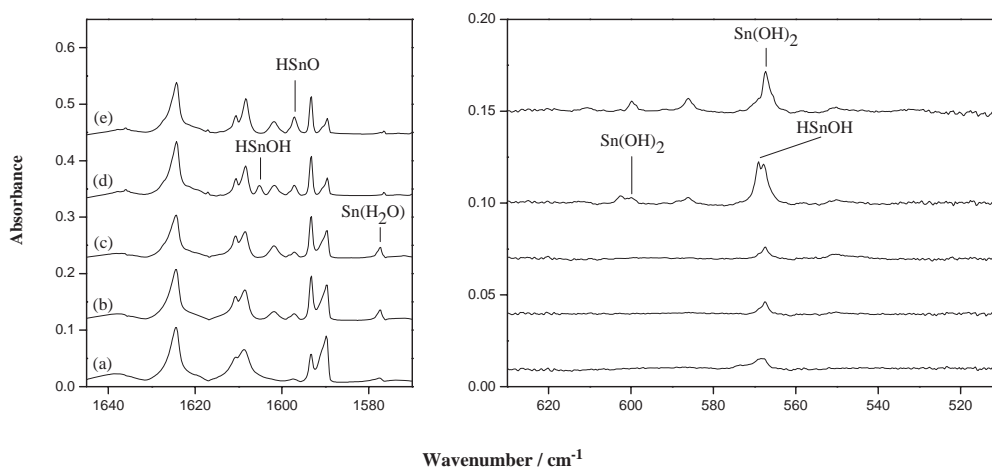


Fig. 4. Infrared spectra in the 1645–1570 and 630–510  $\text{cm}^{-1}$  regions from co-deposition of laser-ablated Sn atoms with 0.2%  $\text{H}_2\text{O}$  in argon: (a) 1 h sample deposition at 4 K; (b) after annealing to 25 K; (c) after annealing to 30 K; (d) after 20 min of broad-band irradiation; (e) after annealing to 35 K.

(Fig. 4). Although this band was observed previously,<sup>5a</sup> here, we present a more detailed discussion. It shifted to 1169.0  $\text{cm}^{-1}$  with  $\text{D}_2\text{O}$  and to 1570.6  $\text{cm}^{-1}$  with  $\text{H}_2^{18}\text{O}$ , giving an isotopic H/D ratio of 1.3494 and  $^{16}\text{O}/^{18}\text{O}$  ratio of 1.0043. No intermediate absorptions were observed in the mixed  $\text{H}_2^{16}\text{O}$  +  $\text{H}_2^{18}\text{O}$  experiments, indicating that only one  $\text{H}_2\text{O}$  subunit is involved in this complex. This band was assigned to the  $\text{H}_2\text{O}$  bending vibration of the  $\text{Sn}(\text{H}_2\text{O})$  complex, which is accord to the previous thermal matrix isolation study in solid argon (1578.0  $\text{cm}^{-1}$ ).<sup>5a</sup>

As shown in Fig. 7, DFT calculations predicted the  $\text{Sn}(\text{H}_2\text{O})$  complex to have an  $^3A''$  electronic ground state with a  $C_s$  structure, which lies 79.5  $\text{kJ mol}^{-1}$  lower in energy than the singlet one. The  $\text{H}_2\text{O}$  bending vibrational frequency was calculated to be 1613.9  $\text{cm}^{-1}$  (Table 3), which should be scaled by 0.9774 (observed frequency divided by calculated frequency) to fit the experimental frequency. As shown in

Table 2, the calculated isotopic frequency ratios are also in agreement with the experimental values.

**HMOH.** In the Pb +  $\text{H}_2\text{O}$  experiment, a new absorption at 1511.0  $\text{cm}^{-1}$  appeared on annealing to 25 K, changed little on broad-band irradiation, and markedly increased on annealing to 30 K (Fig. 1). This band barely shifted with  $\text{H}_2^{18}\text{O}$  but shifted to 1085.4  $\text{cm}^{-1}$  with  $\text{D}_2\text{O}$ . The H/D isotopic ratio of 1.3921 indicates a Pb–H stretching vibrational mode. The doublet feature in the experiment with the  $\text{H}_2\text{O}/\text{HDO}/\text{D}_2\text{O}$  mixture indicates that only one Pb–H subunit is involved (Fig. 3). This band was assigned to the Pb–H stretching vibration of the HPbOH molecule. Two bands at 506.5 and 495.5  $\text{cm}^{-1}$  exhibited the same annealing and irradiation behavior with the 1511.0  $\text{cm}^{-1}$  band, suggesting that these absorptions are due to the different modes of the same molecule. The 506.5  $\text{cm}^{-1}$  band shifted to 480.9  $\text{cm}^{-1}$  with  $\text{H}_2^{18}\text{O}$  (Fig. 2) and to 502.4  $\text{cm}^{-1}$  with  $\text{D}_2\text{O}$ . The  $^{16}\text{O}/^{18}\text{O}$  isotopic ratio of 1.0532

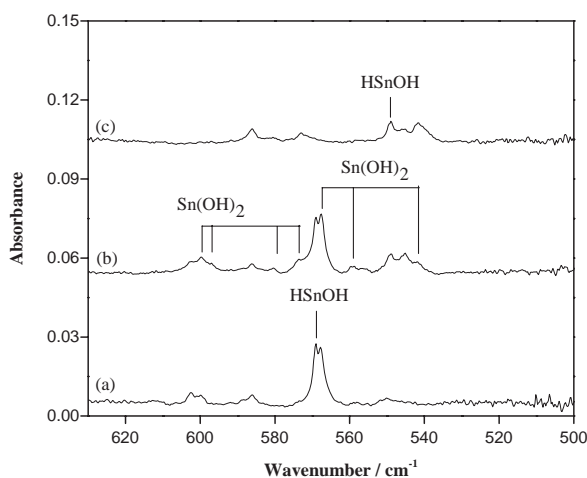


Fig. 5. Infrared spectra in the 630–500  $\text{cm}^{-1}$  regions from co-deposition of laser-ablated Sn atoms with isotopic  $\text{H}_2\text{O}$  in argon: (a) 0.2%  $\text{H}_2\text{O}$ ; (b) 0.2%  $\text{H}_2\text{O}$  + 0.2%  $\text{H}_2^{18}\text{O}$ ; (c) 0.2%  $\text{H}_2^{18}\text{O}$ .

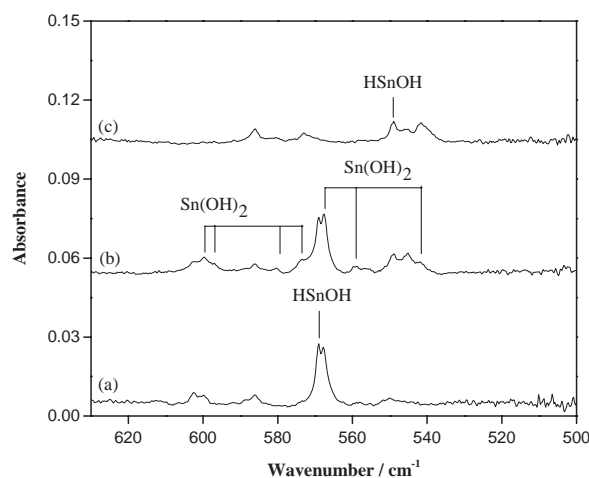


Fig. 6. Infrared spectra in the 1645–1570 and 1173–1140  $\text{cm}^{-1}$  regions from co-deposition of laser-ablated Sn atoms with 0.1%  $\text{H}_2\text{O}$  + 0.2%  $\text{HDO}$  + 0.1%  $\text{D}_2\text{O}$  in argon: (a) 1 h sample deposition at 4 K; (b) after annealing to 25 K; (c) after annealing to 30 K; (d) after 20 min of broad-band irradiation; (e) after annealing to 35 K.

Table 1. Infrared Absorptions ( $\text{cm}^{-1}$ ) from Codeposition of Laser-Ablated Pb and Sn Atoms with  $\text{H}_2\text{O}$  in Excess Argon at 4 K

$\text{H}_2\text{O}$	$\text{D}_2\text{O}$	$\text{H}_2^{18}\text{O}$	H/D	$^{16}\text{O}/^{18}\text{O}$	Assignment
1585.8	1171.7	1579.3	1.3534	1.0041	$\text{Pb}(\text{H}_2\text{O})$ ( $\text{H}_2\text{O}$ bend)
1511.0	1085.4	1511.0	1.3921	1.0000	$\text{HPbOH}$ ( $\text{Pb-H}$ stretch)
1493.8	1070.7	1493.6	1.3952	1.0001	$\text{HPbO}$ ( $\text{Pb-H}$ stretch)
506.5	502.4	480.9	1.0082	1.0532	$\text{HPbOH}$ ( $\text{Pb-OH}$ stretch)
495.5		493.4		1.0043	$\text{HPbOH}$ ( $\text{Pb-O-H}$ deform)
481.2	472.4		1.0186		$\text{PbOH}$ ( $\text{Pb-OH}$ stretch)
1605.5	1157.1	1604.7	1.3875	1.0005	$\text{HSnOH}$ ( $\text{Sn-H}$ stretch)
1597.2	1147.4	1596.9	1.3920	1.0002	$\text{HSnO}$ ( $\text{Sn-H}$ stretch)
1577.4	1169.0	1570.6	1.3494	1.0043	$\text{Sn}(\text{H}_2\text{O})$ ( $\text{H}_2\text{O}$ bend)
569.0	567.6	549.0	1.0025	1.0364	$\text{HSnOH}$ ( $\text{Sn-OH}$ stretch)

and H/D isotopic ratio of 1.0082 suggest that a  $\text{Pb-OH}$  stretching mode is involved. The mixed  $\text{H}_2^{16}\text{O} + \text{H}_2^{18}\text{O}$  isotopic spectra indicated that only one O atom is involved. On the other hand, the band at 495.5  $\text{cm}^{-1}$  slightly shifted (2.1  $\text{cm}^{-1}$ ) with  $\text{H}_2^{18}\text{O}$  and is mainly due to a  $\text{Pb-O-H}$  deforming mode.

Present DFT calculations predicted  $\text{HPbOH}$  to have an  $^1\text{A}'$  electronic ground state with  $\text{C}_s$  symmetry (Fig. 7) and to be the most stable structural isomer of  $\text{Pb-H}_2\text{O}$ . The corresponding triplet one was found to have an imaginary frequency. The  $\text{Pb-H}$ ,  $\text{Pb-OH}$  stretching vibrations and the  $\text{Pb-O-H}$  deforming vibration were calculated to be 1541.4, 492.1, and 519.5  $\text{cm}^{-1}$  (Tables 2 and 3), respectively, which supports for the above assignment. Furthermore, as shown in Table 2, the calculated isotopic frequency ratios are also consistent with the experimental values.

In the  $\text{Sn} + \text{H}_2\text{O}$  experiment, a new band at 1605.5  $\text{cm}^{-1}$  and a band at 569.0  $\text{cm}^{-1}$  appeared after broad-band irradiation, and disappeared on further annealing (Fig. 4). The upper band scarcely shifted with  $\text{H}_2^{18}\text{O}$  but shifted to 1157.1  $\text{cm}^{-1}$  with  $\text{D}_2\text{O}$ , giving a H/D isotopic ratio of 1.3875. This indicates that it is a  $\text{Sn-H}$  stretching vibrational mode. In the

experiment with the  $\text{H}_2\text{O}/\text{HDO}/\text{D}_2\text{O}$  mixture, the doublet feature indicates that only one  $\text{Sn-H}$  subunit is involved (Fig. 6). The lower band shifted to 549.0  $\text{cm}^{-1}$  with  $\text{H}_2^{18}\text{O}$  (Fig. 5) and to 567.6  $\text{cm}^{-1}$  with  $\text{D}_2\text{O}$ . The  $^{16}\text{O}/^{18}\text{O}$  isotopic ratio of 1.0364 and H/D isotopic ratio of 1.0025 imply a  $\text{Sn-OH}$  stretching mode is involved. The doublet feature in the mixed  $\text{H}_2^{16}\text{O} + \text{H}_2^{18}\text{O}$  experiment indicates that only one O atom is involved (Fig. 5).

The  $\text{HSnOH}$  molecule was predicted to have an  $^1\text{A}'$  electronic ground state with a  $\text{C}_s$  symmetry (Fig. 7) and to be the most stable structural isomer of  $\text{Sn-H}_2\text{O}$ . The corresponding triplet one was found to have an imaginary frequency. The  $\text{Sn-H}$  and  $\text{Sn-OH}$  stretching vibrations were calculated to be at 1631.5 and 536.6  $\text{cm}^{-1}$  (Tables 2 and 3), respectively, which supports for the above assignment. Furthermore, as shown in Table 2, the calculated isotopic frequency ratios are also consistent with the experimental values.

**HMO.** In the  $\text{Pb} + \text{H}_2\text{O}$  experiment, a new 1493.8  $\text{cm}^{-1}$  band appeared during sample deposition, visibly increased on sample annealing to 25 K, slightly decreased on broad-band irradiation, and markedly increased on further annealing

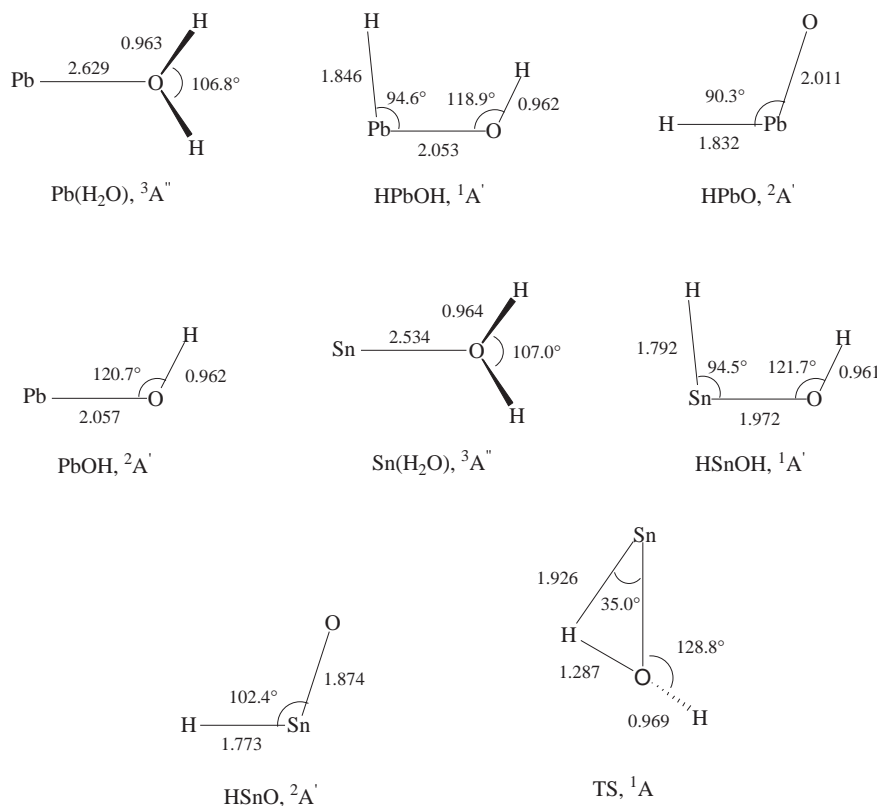


Fig. 7. Optimized structures (bond length in angstroms, bond angle in degrees) of the possible products and the transition states calculated at the B3LYP level.

Table 2. Comparison of Observed and Calculated IR Frequencies and Isotopic Frequency Ratios of the Reaction Products

Molecule	Mode	Freq/cm <sup>-1</sup>		H/D		<sup>16</sup> O/ <sup>18</sup> O	
		obsd	calcd	obsd	calcd	obsd	calcd
Pb(H <sub>2</sub> O)	H <sub>2</sub> O bend	1585.8	1613.3	1.3534	1.3640	1.0041	1.0044
HPbOH	Pb-H stretch	1511.0	1541.4	1.3921	1.4100	1.0000	1.0000
	Pb-OH stretch	506.5	492.1	1.0082	1.0117	1.0532	1.0540
	Pb-O-H deform	495.5	519.5		1.3621	1.0043	1.0043
	Pb-H stretch	1493.8	1530.3	1.3952	1.4100	1.0001	1.0000
PbOH	Pb-OH stretch	481.2	489.3	1.0186	1.0066		1.0552
Sn(H <sub>2</sub> O)	H <sub>2</sub> O bend	1577.4	1613.9	1.3494	1.3638	1.0043	1.0044
HSnOH	Sn-H stretch	1605.5	1631.5	1.3875	1.4074	1.0005	1.0000
	Sn-OH stretch	569.0	536.6	1.0025	0.9902	1.0364	1.0443
HSnO	Sn-H stretch	1597.2	1615.6	1.3920	1.4079	1.0002	1.0000

(Fig. 1). This band barely shifted with H<sub>2</sub><sup>18</sup>O but shifted to 1070.7 cm<sup>-1</sup> with D<sub>2</sub>O. The band position and isotopic frequency ratios (H/D, 1.3952, <sup>16</sup>O/<sup>18</sup>O, 1.0001) suggest that this band is due to a Pb-H stretching vibrational mode. The mixed H<sub>2</sub>O + HDO + D<sub>2</sub>O experiments indicate that only one H atom is involved in this mode (Fig. 3). Accordingly, the 1493.8 cm<sup>-1</sup> band was assigned to the Pb-H stretching vibration of the HPbO molecule.

The HPbO molecule was predicted to have an <sup>2</sup>A' ground state with C<sub>s</sub> symmetry (Fig. 7). The Pb-H and Pb-O stretching vibrations were predicted to be at 1530.3 (381 kmol<sup>-1</sup>) and 471.4 (3 kmol<sup>-1</sup>) cm<sup>-1</sup>, respectively, which is similar to the results recently reported for the reaction of Pb with

H<sub>2</sub>O<sub>2</sub>.<sup>12</sup> The Pb-O stretching vibration of the PbO molecule was observed at 711.2 cm<sup>-1</sup> in solid argon,<sup>19</sup> and the Pb-O stretching vibration of the HPbO molecule is expected to shift to a lower frequency than that of the PbO molecule. The calculated intensity of the Pb-O stretching vibration was too small to be observed, which is consistent with the present experiments.

In the Sn + H<sub>2</sub>O experiment, an absorption at 1597.2 cm<sup>-1</sup> appeared during sample deposition, slightly increased on annealing to 25 and 30 K, visibly increased on broad-band irradiation and markedly increased on annealing to 35 K (Fig. 4). This band barely shifted with H<sub>2</sub><sup>18</sup>O, but shifted to 1147.4 cm<sup>-1</sup>, giving a H/D isotopic ratio of 1.3920, which implies

Table 3. Calculated Vibrational Frequencies and Intensities ( $\text{km mol}^{-1}$ ) of Possible Species Involved in the Pb and Sn +  $\text{H}_2\text{O}$  Reactions (Only the Frequencies Above  $400 \text{ cm}^{-1}$  are Listed)

Species	Elec state	Point group	Frequency/ $\text{cm}^{-1}$ (intensity, mode)
Pb( $\text{H}_2\text{O}$ )	$^3\text{A}''$	$\text{C}_s$	3914.3 (138, $\text{A}''$ ), 3811.3 (62, $\text{A}'$ ), 1613.3 (83, $\text{A}'$ )
HPbOH	$^1\text{A}'$	$\text{C}_s$	3865.6 (54, $\text{A}'$ ), 1541.4 (708, $\text{A}'$ ), 742.6 (27, $\text{A}'$ ), 525.8 (50, $\text{A}'$ ), 519.5 (207, $\text{A}''$ ), 492.1 (149, $\text{A}'$ )
HPbO	$^2\text{A}'$	$\text{C}_s$	1530.3 (381, $\text{A}'$ ), 471.4 (3, $\text{A}'$ )
PbOH	$^2\text{A}'$	$\text{C}_s$	3857.9 (72, $\text{A}'$ ), 629.6 (61, $\text{A}'$ ), 489.3 (131, $\text{A}'$ )
Sn( $\text{H}_2\text{O}$ )	$^3\text{A}''$	$\text{C}_s$	3907.3 (145, $\text{A}''$ ), 3803.4 (64, $\text{A}'$ ), 1613.9 (85, $\text{A}'$ )
HSnOH	$^1\text{A}'$	$\text{C}_s$	3872.7 (57, $\text{A}'$ ), 1631.5 (603, $\text{A}'$ ), 761.1 (53, $\text{A}'$ ), 578.0 (9, $\text{A}'$ ), 540.7 (200, $\text{A}''$ ), 536.6 (194, $\text{A}'$ )
HSnO	$^2\text{A}'$	$\text{C}_s$	1615.6 (199, $\text{A}'$ ), 621.6 (7, $\text{A}'$ )
TS	$^1\text{A}$	$\text{C}_1$	3720.2 (9, $\text{A}$ ), 1519.9 (111, $\text{A}$ ), 624.2 (69, $\text{A}$ ), 475.1 (46, $\text{A}$ ), 311.5 (182, $\text{A}$ ), 1546.0i (2218, $\text{A}$ )

that this band is due to a Sn–H stretching vibrational mode. The doublet feature in the mixed  $\text{H}_2\text{O} + \text{HDO} + \text{D}_2\text{O}$  experiments indicates that only one H atom is involved in this mode (Fig. 6). Accordingly, the  $1597.2 \text{ cm}^{-1}$  band was assigned to the Sn–H stretching vibration of the HSnO molecule; different from the previous report in which a band at  $1597.7 \text{ cm}^{-1}$  has been assigned to the HSnOH molecule.<sup>5a</sup>

The present DFT calculations lend support for the assignment of HSnO. The HSnO molecule was predicted to have an  $^2\text{A}'$  ground state with  $\text{C}_s$  symmetry (Fig. 7). The Sn–H and Sn–O stretching vibrations were predicted to be at  $1615.6 (199 \text{ km mol}^{-1})$  and  $621.6 (7 \text{ km mol}^{-1}) \text{ cm}^{-1}$ , respectively. The calculated intensity of the Sn–O stretching vibration was too small to be observed, which is consistent with the present experimental observation.

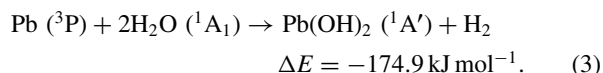
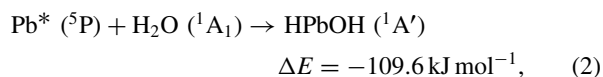
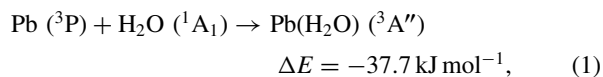
**M(OH)<sub>2</sub>.** In the Pb +  $\text{H}_2\text{O}$  experiment, absorptions at  $707.1$ ,  $533.5$ , and  $502.7 \text{ cm}^{-1}$  appeared during sample deposition, changed little on annealing to  $25 \text{ K}$ , visibly increased after broad-band irradiation, and markedly increased upon further annealing (Fig. 1). These bands were assigned to the Pb(OH)<sub>2</sub> molecule on the basis of a recent report ( $706.8$ ,  $533.5$ , and  $502.7 \text{ cm}^{-1}$ ) on the reaction of Pb and  $\text{H}_2\text{O}_2$ .<sup>12</sup>

In the Sn +  $\text{H}_2\text{O}$  experiment, the absorptions at  $728.0$ ,  $599.9$ , and  $567.8 \text{ cm}^{-1}$  markedly increased after broad-band irradiation and were assigned to the Sn(OH)<sub>2</sub> molecule, based on a recent report ( $727.4$ ,  $598.8$ , and  $565.7 \text{ cm}^{-1}$ ) on the reaction of Sn and  $\text{H}_2\text{O}_2$ .<sup>12</sup>

**Other Absorption.** In the Pb +  $\text{H}_2\text{O}$  experiment, a new weak absorption at  $481.2 \text{ cm}^{-1}$  appeared after broad-band irradiation and changed little on further annealing (Fig. 1). This band shifted to  $472.4 \text{ cm}^{-1}$  with  $\text{D}_2\text{O}$ . The H/D isotopic frequency ratio was  $1.0186$ , implying a Pb–OH stretching vibrational mode. Accordingly, the  $481.2 \text{ cm}^{-1}$  band was tentatively assigned to the Pb–OH stretching vibration of the PbOH molecule. B3LYP calculations predicted the PbOH molecule to

have an  $^2\text{A}'$  ground state with a nonlinear structure (Fig. 7). The calculated Pb–OH stretching vibrational frequency was  $489.3 \text{ cm}^{-1}$  (Table 3), which is in accord with the experimental observations ( $481.2 \text{ cm}^{-1}$ ).

**Reaction Mechanism.** On the basis of the behavior of sample annealing and irradiation together with the observed species and calculated stable isomers, plausible reaction mechanisms are proposed as follows. Under the present experimental conditions, laser-ablated Pb atoms co-deposit with water molecules to form the Pb( $\text{H}_2\text{O}$ ) complex during sample deposition, which slightly increased on annealing and changed little after broadband irradiation. This suggests that the ground state  $^3\text{P}$  Pb atoms can react with water to form the Pb( $\text{H}_2\text{O}$ ) complex spontaneously and the Pb( $\text{H}_2\text{O}$ ) molecule is more stable than M( $\text{H}_2\text{O}$ ) ( $\text{M} = \text{Si}$ ,<sup>5c</sup> Ge,<sup>5d</sup> and Sn), which rearranges after broadband irradiation. This addition reaction is predicted to be exothermic by about  $37.7 \text{ kJ mol}^{-1}$  (reaction 1). The IR absorptions of HPbOH markedly increased on annealing to  $30 \text{ K}$  after broadband irradiation, whereas the IR absorption of Pb( $\text{H}_2\text{O}$ ) barely changed, implying that the HPbOH molecule is not generated from the isomerization of Pb( $\text{H}_2\text{O}$ ). The HPbOH molecule may be formed from the reaction of the excited Pb\* atom generated by the broad-band irradiation with water molecule during further annealing (reaction 2). IR absorptions for HPbO appeared during sample deposition, suggesting that part of the Pb( $\text{H}_2\text{O}$ ) complexes formed during the co-deposition of  $\text{H}_2\text{O}$  with the Pb atoms generated by pulse laser ablation are dissociated to HPbO and H during deposition. The formation of HPbO molecule may be also due to the reactions of excited atoms. Similar features have also been observed in the reactions of group 4 metal atoms with  $\text{H}_2\text{O}$  in solid argon.<sup>8b</sup> Pb(OH)<sub>2</sub> appeared during sample deposition and increased upon annealing, which form by the reaction of Pb with two water molecules (reaction 3), suggesting that the formation of Pb(OH)<sub>2</sub> does not require activation energy.



Laser-ablated Sn atoms co-deposited with water molecules to form the Sn( $\text{H}_2\text{O}$ ) complex during sample deposition (Fig. 4), which slightly increased on annealing, suggesting that the ground state  $^3\text{P}$  Sn atoms can react with water to form the Sn( $\text{H}_2\text{O}$ ) complex spontaneously. This addition reaction is predicted to be exothermic by about  $39.7 \text{ kJ mol}^{-1}$  (reaction 4). IR absorptions for HSnOH appeared after broadband irradiation, while the IR absorption for Sn( $\text{H}_2\text{O}$ ) disappeared, implying that the HSnOH molecule may be generated from the isomerization of Sn( $\text{H}_2\text{O}$ ) (reaction 5) via broad-band irradiation. From the  $^3\text{A}''$  Sn( $\text{H}_2\text{O}$ ) molecule, there is spin crossing leading to the  $^1\text{A}'$  HSnOH molecule. Although this reaction is predicted to be exothermic by  $104.6 \text{ kJ mol}^{-1}$ , it has a  $149.8 \text{ kJ mol}^{-1}$  energy barrier. HSnOH absorptions appeared after broad-band irradiation, suggesting that reaction 5 requires activation



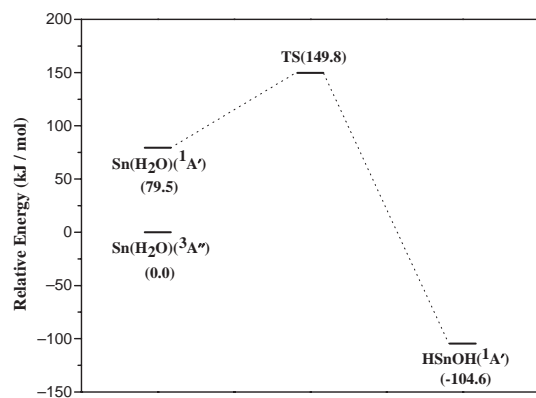
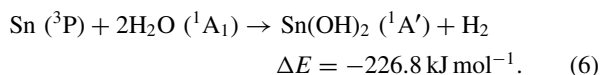
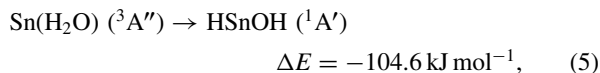
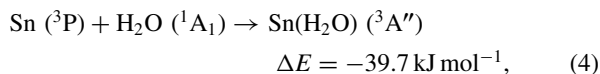


Fig. 8. Potential energy surface following the reaction path from  $\text{Sn}(\text{H}_2\text{O})$  leading to the  $\text{HSnOH}$  product calculated at the B3LYP level. Energies given are in  $\text{kJ mol}^{-1}$  and are relative to  $^3\text{A}''$   $\text{Sn}(\text{H}_2\text{O})$ .

energy (Fig. 8). The IR absorptions of  $\text{HSnO}$  and  $\text{SnO}$  appeared during sample deposition, suggesting that some of the  $\text{Sn}(\text{H}_2\text{O})$  complex formed during the co-deposition of  $\text{H}_2\text{O}$  with the Sn atoms, generated by pulse laser ablation, are dissociated to  $\text{HSnO}$ ,  $\text{SnO}$ ,  $\text{H}$ , or  $\text{H}_2$  during deposition. The formation of these molecules may be due to the reactions of excited atoms, which are produced during laser ablation of the metal target.  $\text{Sn}(\text{OH})_2$  appeared during sample deposition and increased upon annealing, suggesting it forms by the reaction of Sn with two water molecules (reaction 6). This reaction is predicted to be exothermic by  $226.8 \text{ kJ mol}^{-1}$ .



### Conclusion

Reactions of laser-ablated lead and tin atoms with water molecules in argon were studied using matrix-isolation infrared spectroscopy. Adduct and insertion products ( $\text{M}(\text{H}_2\text{O})$ ,  $\text{HMOH}$ , and  $\text{HMO}$ ,  $\text{M} = \text{Pb}$  and  $\text{Sn}$ ) were observed in the present experiments. The products were identified on the basis of the results of the isotopic substitution, step-wise annealing, changes in water concentration and laser energy, and comparison with theoretical predictions.  $\text{Pb}(\text{H}_2\text{O})$  is more stable than  $\text{M}(\text{H}_2\text{O})$  ( $\text{M} = \text{Si}$ ,  $\text{Ge}$ , and  $\text{Sn}$ ), and its isomerization is more difficult than that of  $\text{M}(\text{H}_2\text{O})$  ( $\text{M} = \text{Si}$ ,  $\text{Ge}$ , and  $\text{Sn}$ ). In contrast with the  $\text{HPbOH}$  molecule, the  $\text{HSnOH}$  molecule may form from the isomerization of  $\text{Sn}(\text{H}_2\text{O})$ .

The authors thank the reviewers for valuable suggestions and comments. This work was supported by a Grant-in-Aid for Scientific Research (B) (Grant No. 17350012) from the Ministry of Education, Culture, Sports, Science and Technology (MEXT) of Japan. Y.-L.T. thanks JASSO and Kobe University for Honors Scholarship.

### References

- 1 P. A. Thiel, T. E. Madey, *Surf. Sci. Rep.* **1987**, 7, 211.
- 2 M. A. Henderson, *Surf. Sci. Rep.* **1998**, 46, 1.
- 3 A. Kovalenko, F. Hirata, *J. Chem. Phys.* **1999**, 110, 10095.
- 4 a) B. C. Guo, K. P. Kerns, A. W. Castleman, *J. Phys. Chem.* **1992**, 96, 4879. b) J. L. Tilson, J. F. Harrison, *J. Phys. Chem.* **1991**, 95, 5097. c) Y. M. Chen, D. E. Clemmer, P. B. Armentrout, *J. Phys. Chem.* **1994**, 98, 11490. d) K. Liu, J. M. Parson, *J. Chem. Phys.* **1978**, 68, 1794.
- 5 a) J. W. Kauffman, R. H. Hauge, J. L. Margrave, *ACS Symp. Ser.* **1982**, 179, 355. b) M. A. Douglas, R. H. Hauge, J. L. Margrave, *High Temp. Sci.* **1986**, 22, 47. c) Z. K. Ismail, R. H. Hauge, L. Fredin, J. W. Kauffman, J. L. Margrave, *J. Chem. Phys.* **1982**, 77, 1617. d) Y. L. Teng, L. Jiang, S. Han, Q. Xu, *J. Phys. Chem. A*, in press.
- 6 a) J. W. Kauffman, R. H. Hauge, J. L. Margrave, *J. Phys. Chem.* **1985**, 89, 3541. b) J. W. Kauffman, R. H. Hauge, J. L. Margrave, *J. Phys. Chem.* **1985**, 89, 3547.
- 7 a) L. N. Zhang, J. Dong, M. F. Zhou, *J. Phys. Chem. A* **2000**, 104, 8882. b) L. N. Zhang, L. M. Shao, M. F. Zhou, *Chem. Phys.* **2001**, 272, 27.
- 8 a) M. F. Zhou, J. Dong, L. N. Zhang, Q. Z. Qin, *J. Am. Chem. Soc.* **2001**, 123, 135. b) M. F. Zhou, L. N. Zhang, J. Dong, Q. Z. Qin, *J. Am. Chem. Soc.* **2000**, 122, 10680.
- 9 a) M. F. Zhou, L. N. Zhang, L. M. Shao, W. N. Wang, K. N. Fan, Q. Z. Qin, *J. Phys. Chem. A* **2001**, 105, 5801. b) L. N. Zhang, M. F. Zhou, L. M. Shao, W. N. Wang, K. N. Fan, Q. Z. Qin, *J. Phys. Chem. A* **2001**, 105, 6998.
- 10 J. Xu, M. F. Zhou, *J. Phys. Chem. A* **2006**, 110, 10575.
- 11 a) B. Y. Liang, L. Andrews, J. Li, B. E. Bursten, *J. Am. Chem. Soc.* **2002**, 124, 6723. b) B. Y. Liang, R. D. Hunt, G. P. Kushto, L. Andrews, J. Li, B. E. Bursten, *Inorg. Chem.* **2005**, 44, 2159.
- 12 X. F. Wang, L. Andrews, *J. Phys. Chem. A* **2005**, 109, 9013.
- 13 a) M. F. Zhou, L. Andrews, C. W. Bauschlicher, Jr., *Chem. Rev.* **2001**, 101, 1931. b) H. J. Himmel, A. J. Downs, T. M. Greene, *Chem. Rev.* **2002**, 102, 4191, and references therein.
- 14 a) T. R. Burkholder, L. Andrews, *J. Chem. Phys.* **1991**, 95, 8697. b) M. F. Zhou, N. Tsumori, L. Andrews, Q. Xu, *J. Phys. Chem. A* **2003**, 107, 2458. c) L. Jiang, Q. Xu, *J. Chem. Phys.* **2005**, 122, 034505. d) L. Jiang, Q. Xu, *J. Am. Chem. Soc.* **2005**, 127, 42. e) L. Jiang, Q. Xu, *J. Am. Chem. Soc.* **2005**, 127, 8906. f) Q. Xu, L. Jiang, N. Tsumori, *Angew. Chem., Int. Ed.* **2005**, 44, 4338.
- 15 M. J. Frisch, G. W. Trucks, H. B. Schlegel, G. E. Scuseria, M. A. Robb, J. R. Cheeseman, J. A. Montgomery, Jr., T. Vreven, K. N. Kudin, J. C. Burant, J. M. Millam, S. S. Iyengar, J. Tomasi, V. Barone, B. Mennucci, M. Cossi, G. Scalmani, N. Rega, G. A. Petersson, H. Nakatsuji, M. Hada, M. Ehara, K. Toyota, R. Fukuda, J. Hasegawa, M. Ishida, T. Nakajima, Y. Honda, O. Kitao, H. Nakai, M. Klene, X. Li, J. E. Knox, H. P. Hratchian, J. B. Cross, C. Adamo, J. Jaramillo, R. Gomperts, R. E. Stratmann, O. Yazyev, A. J. Austin, R. Cammi, C. Pomelli, J. W. Ochterski, P. Y. Ayala, K. Morokuma, G. A. Voth, P. Salvador, J. J. Dannenberg, V. G. Zakrzewski, S. Dapprich, A. D. Daniels, M. C. Strain, O. Farkas, D. K. Malick, A. D. Rabuck, K. Raghavachari, J. B. Foresman, J. V. Ortiz, Q. Cui, A. G. Baboul, S. Clifford, J. Cioslowski, B. B. Stefanov, G. Liu, A. Liashenko, P. Piskorz, I. Komaromi, R. L. Martin, D. J. Fox, T. Keith, M. A. Al-Laham, C. Y. Peng, A. Nanayakkara, M. Challacombe,

P. M. W. Gill, B. Johnson, W. Chen, M. W. Wong, C. Gonzalez, J. A. Pople, *Gaussian 03, Revision B.04*, Gaussian, Inc., Pittsburgh, PA, **2003**.

16 a) C. Lee, E. Yang, R. G. Parr, *Phys. Rev. B* **1988**, 37, 785.  
b) A. D. Becke, *J. Chem. Phys.* **1993**, 98, 5648.

17 a) J. H. Wachters, *J. Chem. Phys.* **1970**, 52, 1033. b) P. J.

Hay, *J. Chem. Phys.* **1977**, 66, 4377. c) P. J. Hay, W. R. Wadt, *J. Chem. Phys.* **1985**, 82, 299.

18 Q. Xu, L. Jiang, *Inorg. Chem.* **2006**, 45, 5785.

19 G. V. Chertihin, L. Andrews, *J. Chem. Phys.* **1996**, 105, 2561.